Tipping in Climate Impact Models

Dr. Emmanuel Fleurantin, Dr. Christopher K.R.T. Jones, Martha Hartt, Joanna Ro, Aidan Self, Dimitri Shatov

Mason Experimental Geometry Lab

Fall 2022

Thermohaline Circulation

Thermohaline Circulation

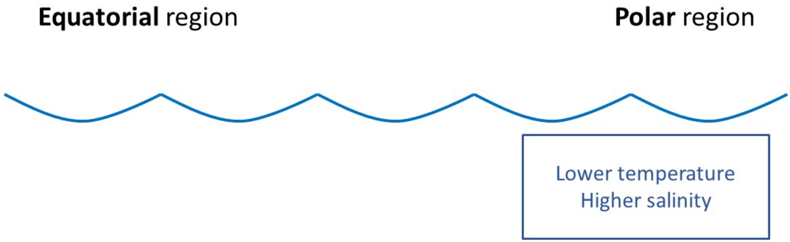

Thermohaline Circulation

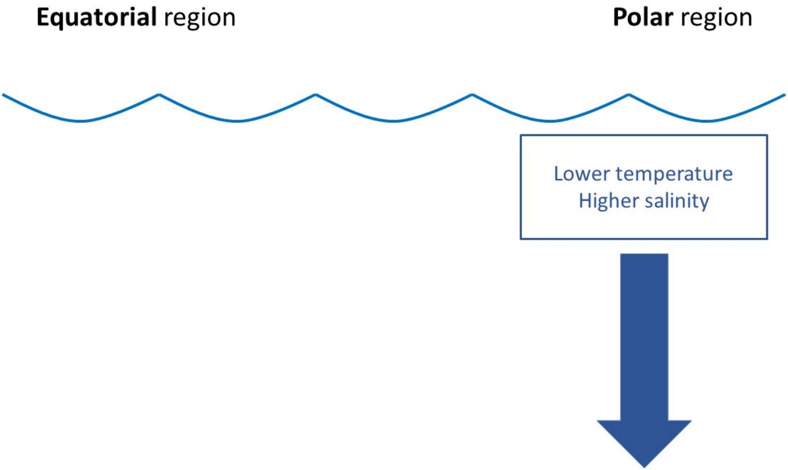

Thermohaline Circulation

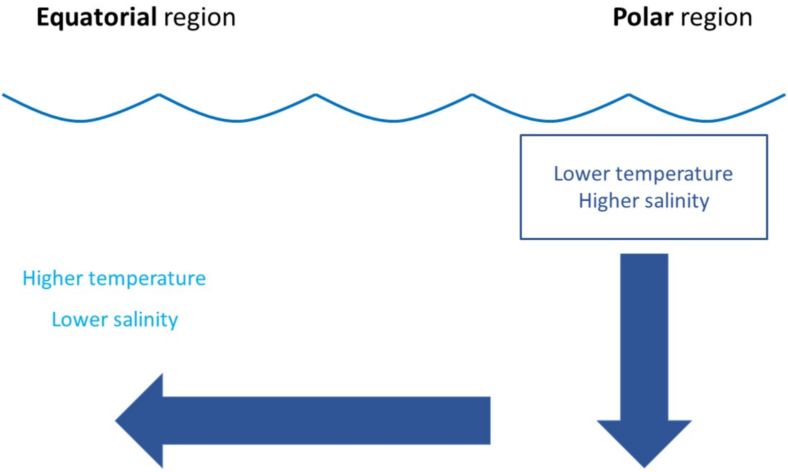

Thermohaline Circulation

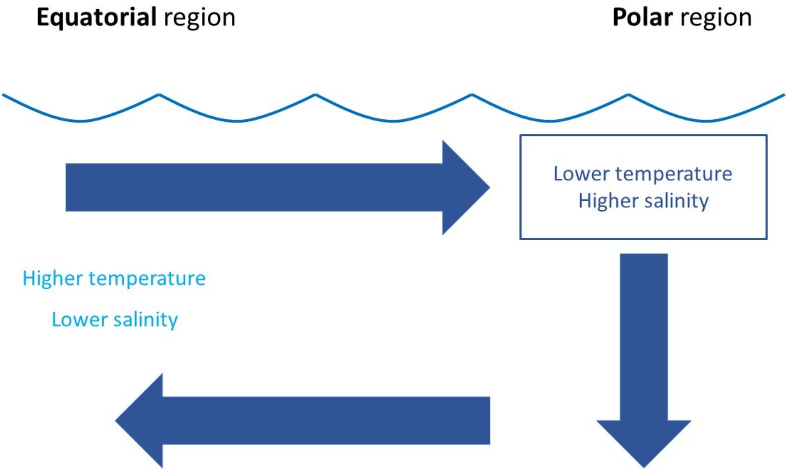

The Stommel Model

[?]

equatorial box

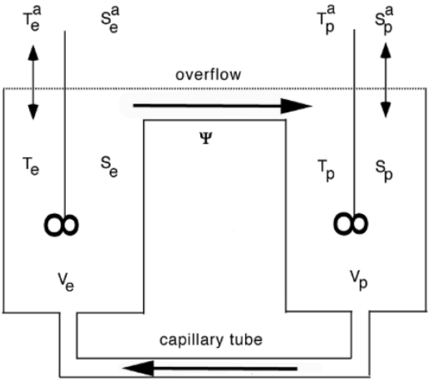

polar box

The Stommel Model

[?]

equatorial box

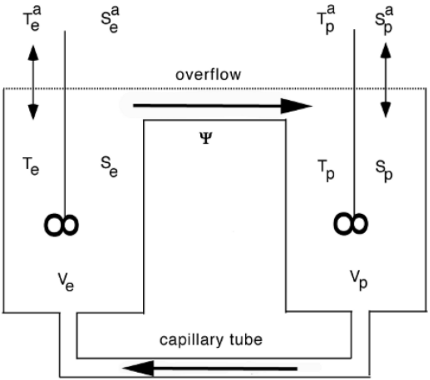

polar box

Flow Rate

$$\Psi_* = \gamma \frac{\rho_{p*} - \rho_{e*}}{\rho_0}$$

Equation of State

$$\rho_* = \rho_0(1 - \alpha_T(T_* - T_0) + \alpha_S(S_* - S_0))$$

A 4-Dimensional System:

$$V_e \frac{dT_{e*}}{dt_*} = C_e^T (T_e^a - T_{e*}) + |\Psi_*|(T_{p*} - T_{e*})$$

$$V_e \frac{dS_{e*}}{dt_*} = C_e^S (S_e^a - S_{e*}) + |\Psi_*|(S_{p*} - S_{e*})$$

$$V_p \frac{dT_{p*}}{dt_*} = C_p^T (T_p^a - T_{p*}) + |\Psi_*|(T_{e*} - T_{p*})$$

$$V_p \frac{dS_{p*}}{dt_*} = C_p^S (S_p^a - S_{p*}) + |\Psi_*|(S_{e*} - S_{p*})$$

A 4-Dimensional System:

$$V_e \frac{dT_{e*}}{dt_*} = C_e^T (T_e^a - T_{e*}) + |\Psi_*|(T_{p*} - T_{e*})$$

$$V_e \frac{dS_{e*}}{dt_*} = C_e^S (S_e^a - S_{e*}) + |\Psi_*|(S_{p*} - S_{e*})$$

$$V_p \frac{dT_{p*}}{dt_*} = C_p^T (T_p^a - T_{p*}) + |\Psi_*|(T_{e*} - T_{p*})$$

$$V_p \frac{dS_{p*}}{dt_*} = C_p^S (S_p^a - S_{p*}) + |\Psi_*|(S_{e*} - S_{p*})$$

$$T = T_e - T_p \,, \quad S = S_e - S_p.$$

[?]

The Stommel System

Nondimensional equations: [?]

$$\frac{dT}{dt} = \eta_1 - T(1 + |T - S|)$$

$$\frac{dS}{dt} = \eta_2 - S(\eta_3 + |T - S|)$$

$$\eta_1 = \frac{(T_e^a - T_p^a)\gamma\alpha_T(V_e + V_p)}{V_e V_p R_T}$$

$$\eta_2 = \frac{R_S}{R_T}\frac{(S_e^a - S_p^a)\gamma\alpha_S(V_e + V_p)}{V_e V_p R_T}$$

$$\eta_3 = \frac{R_S}{R_T}$$

The Stommel System

Nondimensional equations: [?]

$$\frac{dT}{dt} = \eta_1 - T(1 + |T - S|)$$

$$\frac{dS}{dt} = \eta_2 - S(\eta_3 + |T - S|)$$

Equilibrium solutions

$$T = \frac{\eta_1}{1 + |\Psi|} \qquad \text{and} \qquad S = \frac{\eta_2}{\eta_3 + |\Psi|}$$

Periodic Solutions in the Stommel Model

Applying **Bendixson Dulac Theorem** to construct a C^1 dulac function $\varphi(T, S)$ such that the expression:

$$\frac{\partial(\varphi f)}{\partial T} + \frac{\partial(\varphi g)}{\partial S}$$

Has the same sign everywhere ($\neq 0$)
It is worth noting that in our current climate, $T, S \geq 0$ but the proof provided can easily be carried through for $(T, S) \in R^2$ using the same arguments.
Thus we have this theorem:

Theorem

For $T, S \geq 0$, the Stommel model has no periodic solutions.

The Stommel system can be represented by

$$f(T,S) = \frac{dT}{dt} = \eta_1 - T(1 + |T - S|)$$
$$g(T,S) = \frac{dS}{dt} = \eta_2 - S(\eta_3 + |T - S|),$$

where $T, S \geq 0$, and η_1, η_2, η_3 are fixed parameter values. We set $0 < \eta_3 < 1$.
Let $\phi(x,y) = 1$ be our Dulac function.
For $T \neq S$, we have

$$\begin{aligned}\frac{\partial(\phi f)}{\partial T} + \frac{\partial(\phi g)}{dS} &= -1 - |T - S| - T\frac{T-S}{|T-S|} - \eta_3 - |T - S| + S\frac{T-S}{|T-S|} \\ &= -1 - \eta_3 - 2|T-S| + (S - T)\frac{T-S}{|T-S|} \\ &= -1 - \eta_3 - 2|T-S| - \frac{(T-S)^2}{|T-S|}.\end{aligned} \tag{1}$$

Since $0 < \eta_3 < 1$, if $T > S$ or $T < S$, we have $\frac{\partial(\phi f)}{\partial T} + \frac{\partial(\phi g)}{dS} < 0$, so by the Bendixson-Dulac theorem, there are no periodic orbits for

$$\tilde{D}_1 \subset \{(T, S) \in \mathbb{R}^2_+ | T > S\}$$

and

$$\tilde{D}_2 \subset \{(T, S) \in \mathbb{R}^2_+ | S > T\}.$$

Now, we consider all $T, S \geq 0$.
Suppose that there exists a periodic solution C which encloses a region D for all $T, S \geq 0$.

Periodic Solutions in the Stommel Model

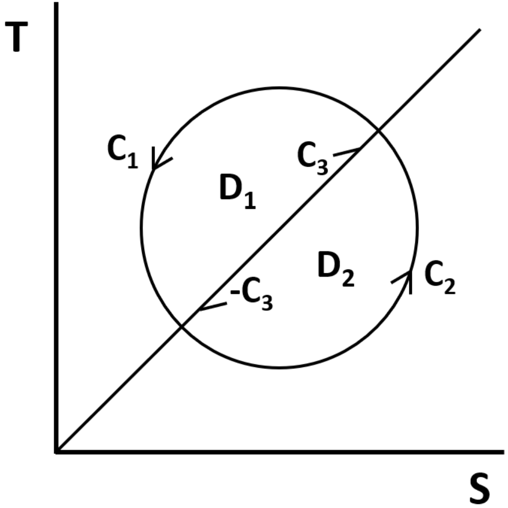

Periodic Solutions in the Stommel Model

$$\iint_D \left(\frac{\partial(\phi f)}{\partial T} + \frac{\partial(\phi g)}{dS} \right) dTdS$$

$$= \iint_{D_1} \left(\frac{\partial(\phi f)}{\partial T} + \frac{\partial(\phi g)}{dS} \right) dTdS + \iint_{D_2} \left(\frac{\partial(\phi f)}{\partial T} + \frac{\partial(\phi g)}{dS} \right) dTdS$$

$$= \oint_{C_1} (-gdT + fdS) + \oint_{C_3} (-gdT + fdS) + \oint_{C_2} (-gdT + fdS) + \oint_{-C_3} (-gdT + fdS)$$

$$= \oint_{C_1} (-gdT + fdS) + \oint_{C_2} (-gdT + fdS) \qquad [\text{recall } \phi = 1]$$

Periodic Solutions in the Stommel Model

$$\begin{aligned}
\iint_D \left(\frac{\partial(\phi f)}{\partial T} + \frac{\partial(\phi g)}{dS} \right) dTdS &= \oint_{C_1} (-gdT + fdS) + \oint_{C_2} (-gdT + fdS) \\
&= \oint_C (-gdT + fdS) \\
&= \oint_C \begin{pmatrix} -g \\ f \end{pmatrix} \cdot \begin{pmatrix} dT \\ dS \end{pmatrix} \\
&= \int_{t=a}^{t=b} \begin{pmatrix} -g(T(t), S(t)) \\ f(T(t), S(t)) \end{pmatrix} \cdot \begin{pmatrix} \frac{dT}{dt} \\ \frac{dS}{dt} \end{pmatrix} dt \\
&= \int_{t=a}^{t=b} \begin{pmatrix} -\frac{dS}{dt} \\ \frac{dT}{dt} \end{pmatrix} \cdot \begin{pmatrix} \frac{dT}{dt} \\ \frac{dS}{dt} \end{pmatrix} dt \\
&= 0\,,
\end{aligned}$$

a contradiction.

Periodic Solutions in the Stommel Model

$\iint\limits_{D} \left(\frac{\partial(\phi f)}{\partial T} + \frac{\partial(\phi g)}{dS} \right) dTdS = 0$ is a contradiction since

$$\iint\limits_{D_1} \left(\frac{\partial(\phi f)}{\partial T} + \frac{\partial(\phi g)}{dS} \right) dTdS + \iint\limits_{D_2} \left(\frac{\partial(\phi f)}{\partial T} + \frac{\partial(\phi g)}{dS} \right) dTdS < 0,$$

using (1), the Bendixson-Dulac theorem for D_1 and D_2.
Thus, we can conclude that the Stommel system has no periodic solutions for any $T, S \geq 0$.
Q.E.D

Steady States

Equilibrium solutions

$$T = \frac{\eta_1}{1 + |\Psi|} \qquad \text{and} \qquad S = \frac{\eta_2}{\eta_3 + |\Psi|}$$

Steady States

Equilibrium solutions

$$T = \frac{\eta_1}{1 + |\Psi|} \qquad \text{and} \qquad S = \frac{\eta_2}{\eta_3 + |\Psi|}$$

TH Regime

If $|\Psi| = \Psi$,

$$\eta_2 = -\Psi^2 - \eta_3 \Psi + \eta_1 \left(\frac{\eta_3 + \Psi}{1 + \Psi} \right)$$

Steady States

Equilibrium solutions

$$T = \frac{\eta_1}{1 + |\Psi|} \qquad \text{and} \qquad S = \frac{\eta_2}{\eta_3 + |\Psi|}$$

TH Regime

If $|\Psi| = \Psi$,

$$\eta_2 = -\Psi^2 - \eta_3 \Psi + \eta_1 \left(\frac{\eta_3 + \Psi}{1 + \Psi} \right)$$

SA Regime

If $|\Psi| = -\Psi$,

$$\eta_2 = \Psi^2 - \eta_3 \Psi + \eta_1 \left(\frac{\eta_3 - \Psi}{1 - \Psi} \right)$$

Steady States

Fix η_1, η_3 such that $\eta_3 < 1$ and $\eta_1 > \dfrac{\eta_3}{1-\eta_3}$.

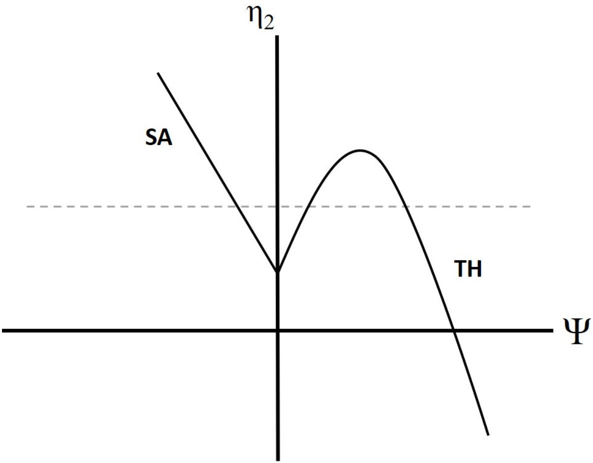

Bifurcation View

For η_1, η_3 fixed such that $\eta_3 < 1$ and $\eta_1 > \dfrac{\eta_3}{1-\eta_3}$

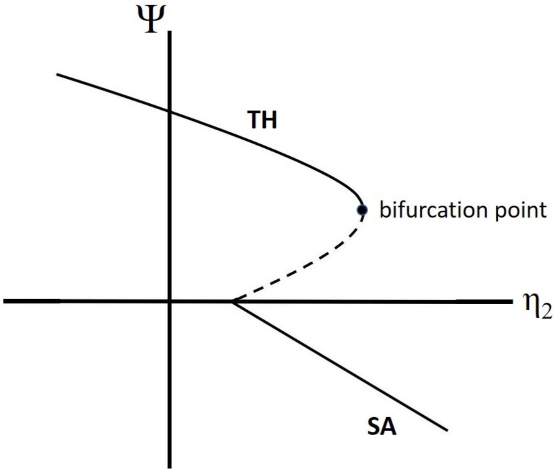

B-Tipping

- Bifurcation induced tipping is a sudden transition
- Occurs with a slow change to an underlying parameter of dynamical system
- Can reduce stability and untimately destroy a stable node
- Analagous to "jumping off a cliff"

R-Tipping

$$\dot{x} = f(x, \lambda)$$

$$\lambda = \Lambda(rt)$$

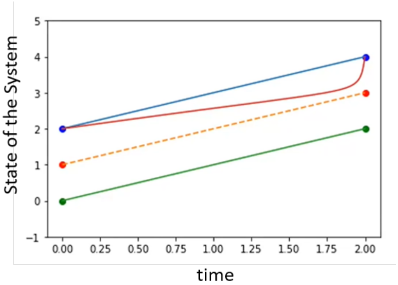

$r < r_c$

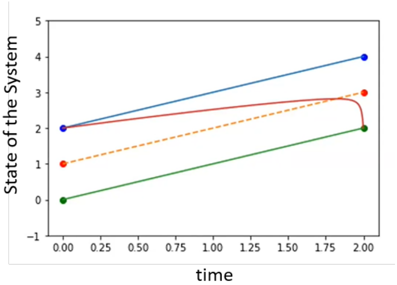

$r > r_c$

[?]

N-Tipping

- Noise Induced Tipping
- Can be characterized by a ball in two valleys on a potential graph
- Noise / "random perturbations" / "Stochastic Process" are responsible for driving a ball from one valley to the next
- The depth of graph determines the amount of noise needed to shift along the graph
- This tipping does not change the original landscape of potential graph

Importance of Tipping

- Tipping is important in our dynamical system because we can examine real world data/parameters
- This can have a direct impact to Earth's Climate thermohaline circulation
- Such as a change in direction of the ocean current's
- Similarly Earth's climate can also induce tipping for the dynamical ocean system.

Data Assimilation

Data assimilation is the process of combining mathematical models with observational data in order to get accurate estimations about the state of a system. DA relies upon state estimation techniques such as the Ensemble Kalman Filter to get accurate predictions.

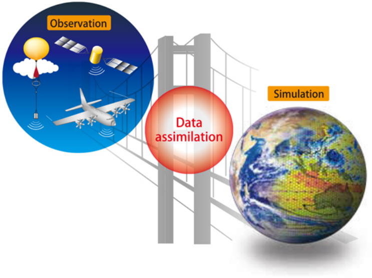

Kalman Filter

The Kalman filter is a two step-process for optimally estimating the state of a linear system. The two steps are the prediction step and the update step. In order to get an optimal prediction, the Kalman filter must maintain and do operations on the covariance matrices for the two Gaussian distributions used to model our prediction and observation.

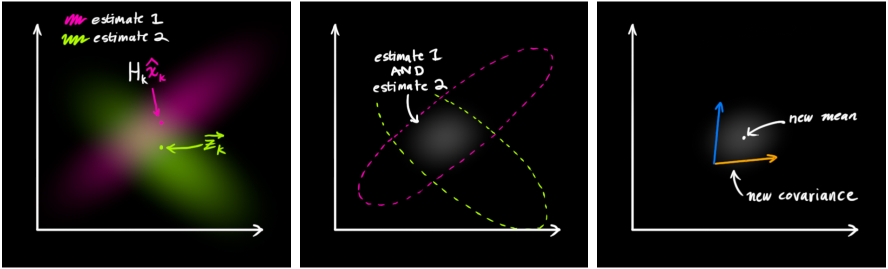

The Kalman Gain Matrix

We have a prediction $\mathcal{N}(\vec{\mu_0}, \Sigma_0)$, and an observation $\mathcal{N}(\vec{\mu_1}, \Sigma_1)$. We want $\mathcal{N}(\vec{\mu_0}, \Sigma_0) \cdot \mathcal{N}(\vec{\mu_1}, \Sigma_1) = \mathcal{N}(\vec{\mu}', \Sigma')$. Using algebra we can get

$$\begin{aligned} \vec{\mu}' &= \vec{\mu_0} + K(\vec{\mu_1} - \vec{\mu_0}) \\ \Sigma' &= \Sigma_0 - K\Sigma_0 \end{aligned} \tag{2}$$

Where K is the Kalman Gain matrix, a parameter that quantifies our confidence in our observation using the covariance matrices Σ_0 and Σ_1.

$$K = \Sigma_0(\Sigma_0 + \Sigma_1)^{-1} \tag{3}$$

Problem solved?

Ensemble Kalman Filter

Problem!

What if our system has billions of state variables? Finding Σ' doesn't look so fun anymore. Also, the Kalman filter doesn't work if our system is nonlinear or models errors using non Gaussian distributions.

New Approach: Monte Carlo Simulation

Estimate the mean and covariance using a set of ensemble members (multiple state vectors).

Additional Benefits:

- Model is treated as black box
- Highly parallelizable

DAPPER

DAPPER is a set of methods for benchmarking the performance of different data assimilation techniques. It does this by running a "twin experiment", where a synthetic truth is created and then used as a optimal reference point to compare different DA methods. Our implementation of the Stommel model relies on this library.

Observation Sources

Table: Parameters, forcings, initial conditions and their sources for our simulations for the Stommel model.

Data	Values	Source	Details
Temperature (ocean temperature)	Pole: 6C, Equator: 18C	[1]	1981-2010, annual, 200m depth
Salt (ocean salinity)	Pole: 35ppt Equator: 36.5ppt	[2]	1981-2010, annual, 200m depth
temp_diff (surface heat mixing coefficient)	$\frac{\kappa_T}{z_{\text{mixing}}}$ with $\kappa_T = 10^{-4}\mathrm{ms}^{-1}$	[3]	
salt_diff (surface salinity mixing coefficient)	$\frac{\kappa_S}{z_{\text{mixing}}}$ with $\kappa_S = \eta_3 \kappa_T$	[4]	$\eta_3 = 0.3$
z_{mixing} (mixing layer depth)	50m	[5]	2005-2017, annual, surface value at 20N
dx (width North-Atlantic basin in lateral direction)	4800 km	[6]	
dy (width North-Atlantic basin in longitudinal direction)	5200 km	[7]	
dz (depth North-Atlantic basin)	3650 m	[6]	
rho_ref (reference density)	1027 kgm^{-3}	[8]	
S_ref (reference salinity)	35 ppt	[8]	
T_ref (reference temperature)	10 C	[8]	
α_T (thermal expansion coefficient)	$\frac{0.15K^{-1}}{\rho_{\text{ref}}}$	[8]	
α_S (haline expansion coefficient)	$\frac{0.78ppt^{-1}}{\rho_{\text{ref}}}$	[8]	
Q_overturning (meridional overturning flux))	18 Sv	[9]	
γ (advective transport coefficient)	$\frac{\rho_{\text{ref}}}{\rho_p - \rho_e} \frac{\text{Q\_overturning}}{dxdz}$		ρ_p and ρ_e computed using initial conditions
temp_air	Pole: 8.5C, Equator: 26C	[1]	1981-2010, annual, surface.
salt_air	Pole: 32.8ppt, Equator: 36.6ppt	[2]	1981-2010, annual, surface depth
V_ice	$3.42 \times 10^6 km^3$	[10]	Area (1,710,000 km^2) times thickness (2 km)
T_ice	100 years		
T_warming	100 years		
avg_temp_warming (global warming)	3C	[11, 12]	
diff_temp_warming (half difference warming pole vs. equator)	6C	[13]	

Reference Ensemble Run

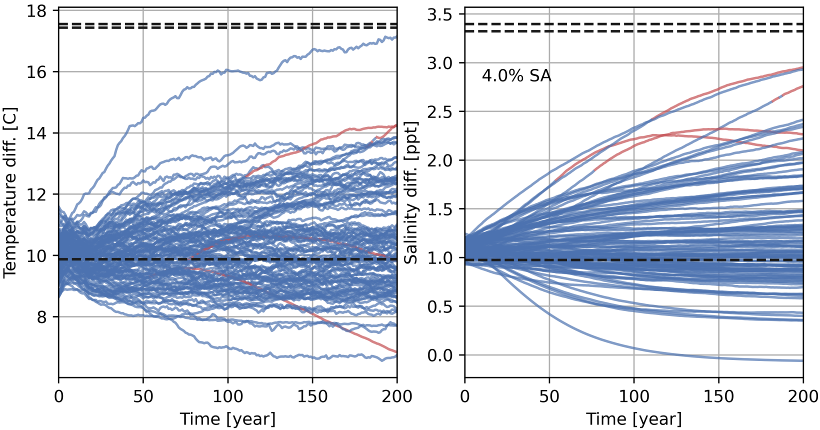

Reference Ensemble Run + DA

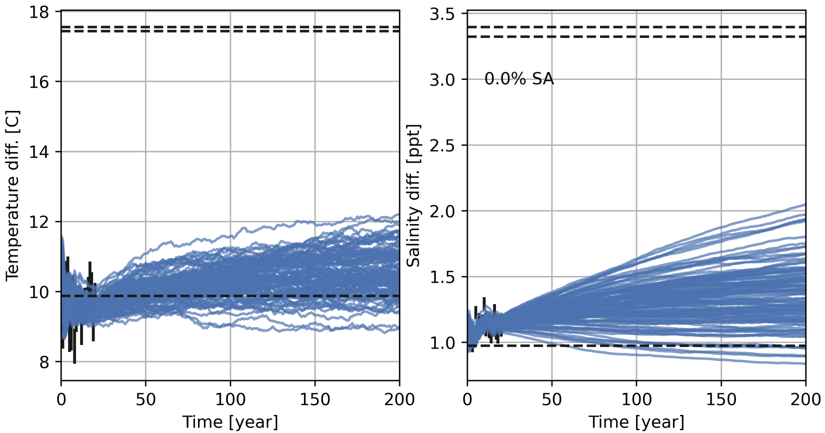

Effect of Global Warming

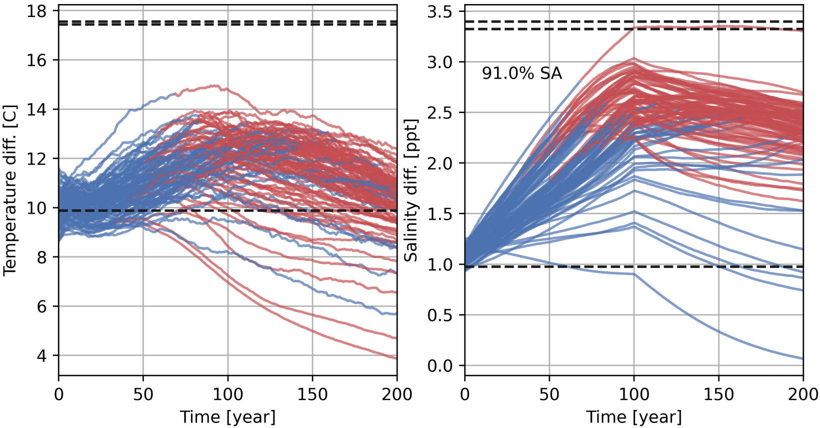

Effect of Global Warming + DA

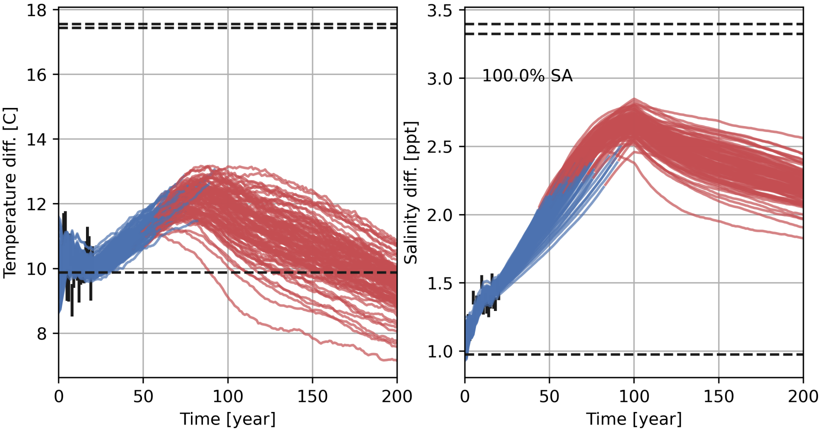

Conclusions

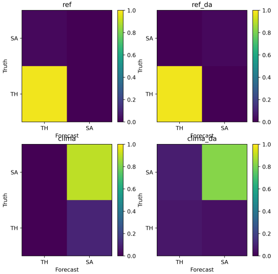

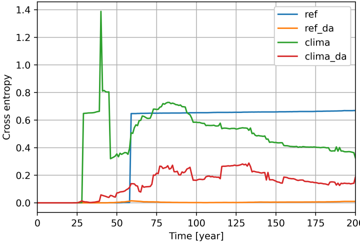

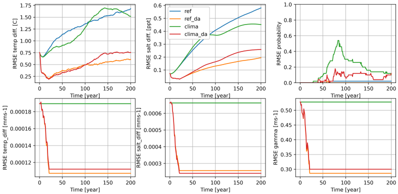

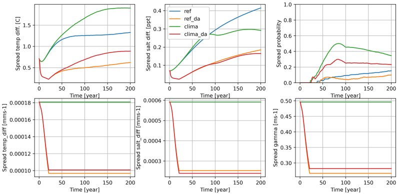

Conclusions

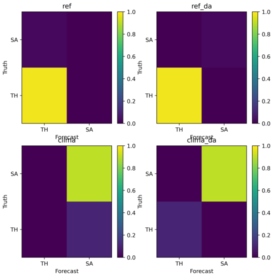

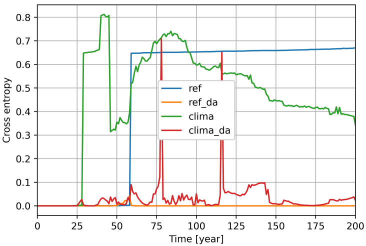

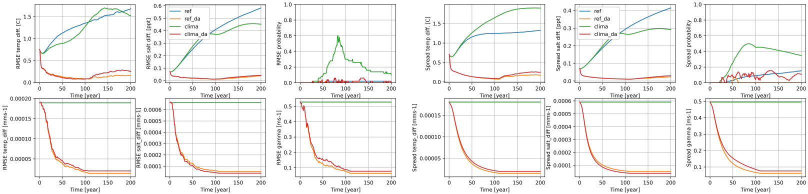

Conclusions

- We used the Stommel 2-box model to reproduce meridional overturning circulation.
- Our simulations confirmed that melting of the Greenland ice sheet and north pole can cause a regime change from TH to SA.
- Assimilating data from more years of observation significantly reduces the spread of ensemble members over time.
- Model should be continually updated as more data becomes available.

References I

[1] National centers for environmental information (ncei).
URL https://www.ncei.noaa.gov/access/world-ocean-atlas-2018f/bin/woa18f.pl?parameter=s.
Last accessed 2022-11-21.

[2] National centers for environmental information (ncei).
URL https://www.ncei.noaa.gov/access/world-ocean-atlas-2018f/bin/woa18f.pl?parameter=t.
Last accessed 2022-11-21.

[3] Lynne D. Talley, George L. Pickard, William J. Emery, and James H. Swift.
Descriptive Physical Oceanography (Sixth Edition).
Academic Press, Boston, sixth edition edition, 2011.

[4] Henk A. Dijkstra.
Dynamical Oceanography.
Springer Berlin,, Heidelberg, 1st edition edition, 2011.

References II

[5] National centers for environmental information (ncei).
URL https://www.ncei.noaa.gov/access/world-ocean-atlas-2018f/bin/woa18f.pl?parameter=M.
Last accessed 2022-11-21.

[6] Atlantic ocean.
URL https://www.britannica.com/place/Atlantic-Ocean.
Last accessed 2022-11-21.

[7] Department of defense world geodetic system 1984, its definition and relationships with local geodetic systems.
URL https://apps.dtic.mil/sti/pdfs/ADA280358.pdf.
Last accessed 2022-11-21.

[8] Jonas Nycander, Magnus Hieronymus, and Fabien Roquet.
The nonlinear equation of state of sea water and the global water mass distribution.
Geophysical Research Letters, 42(18):7714–7721, 2015.

References III

[9] G.D. McCarthy, D.A. Smeed, W.E. Johns, E. Frajka-Williams, B.I. Moat, D. Rayner, M.O. Baringer, C.S. Meinen, J. Collins, and H.L. Bryden. Measuring the atlantic meridional overturning circulation at 26°n. *Progress in Oceanography*, 130:91–111, 2015.

[10] Greenland ice sheet. URL https://en.wikipedia.org/wiki/Greenland_ice_sheet. Last accessed 2022-11-21.

[11] Climate change: Global temperature projections. URL https://www.climate.gov/news-features/understanding-climate/climate-change-global-temperature-projections. Last accessed 2022-11-21.

References IV

[12] Climate change 2007: Synthesis report.
URL https://www.ipcc.ch/site/assets/uploads/2018/02/ar4_syr_full_report.pdf.
Last accessed 2022-11-21.

[13] Jinlun Zhang.
Warming of the arctic ice-ocean system is faster than the global average since the 1960s.
Geophysical Research Letters, 32(19), 2005.